

General predictions for the neutron star crustal moment of inertia

Thomas Carreau,¹ Francesca Gulminelli,¹ and Jérôme Margueron²

¹CNRS, ENSICAEN, UMR6534, LPC, F-14050 Caen cedex, France

²Institut de Physique Nucléaire de Lyon, CNRS/IN2P3, Université de Lyon, Université Claude Bernard Lyon 1, F-69622 Villeurbanne cedex, France

(Dated: March 3, 2022)

The neutron star crustal EoS and transition point properties are computed within a unified meta-modeling approach. A Bayesian approach is employed including two types of filters: bulk nuclear properties are controlled from low density effective field theory (EFT) predictions as well as the present knowledge from nuclear experiments, while the surface energy is adjusted on experimental nuclear masses. Considering these constraints, a quantitative prediction of crustal properties can be reached with controlled confidence intervals and increased precision with respect to previous calculations: $\approx 11\%$ dispersion on the crustal width and $\approx 27\%$ dispersion on the fractional moment of inertia. The crust moment of inertia is also evaluated as a function of the neutron star mass, and predictions for mass and radii are given for different pulsars. The possible crustal origin of Vela pulsar glitches is discussed within the present estimations of crustal entrainment, disfavoring a large entrainment phenomenon if the Vela mass is above $1.4M_{\odot}$. Further refinement of the present predictions requires a better estimation of the high order isovector empirical parameters, e.g. K_{sym} and Q_{sym} , and a better control of the surface properties of extremely neutron rich nuclei.

The standard theory of pulsar glitches, this sudden spin-up of the rotational frequency of a compact star observed in almost 200 different pulsars since their discovery [1], assumes that the observed phenomenon originates from an abrupt transfer of angular momentum from the neutron superfluid to the solid crust of the star, due to the unpinning of the superfluid vortices from the crystal lattice [2]. For this mechanism to justify the large glitches observed in some pulsars such as Vela, the neutron star crust must be sufficiently thick to store a significant amount of angular momentum. The corresponding fraction of crust moment of inertia I_{crust}/I can be estimated [3–5] in a range going from 1.6 % up to 15 %, depending on the importance of the effect of crustal entrainment, which is currently under debate [6, 7].

A reliable estimation of the crust thickness and of the associated moment of inertia is therefore crucially needed to validate the crustal origin of pulsar glitches. This quantity is also a key parameter for the simulations of neutron star cooling [8]. For this estimation, constraints from low energy nuclear physics appear more promising than direct constraints from astrophysics [9, 10]. Indeed, the only poorly known parameter for the determination of the crustal thickness of a neutron star is the nuclear EoS and, most important, the density and pressure at the transition point from the solid crust to the liquid core [11].

In this Letter, we present a unified EoS treatment [12–14], where the core and crust EoS are built within the same functional. To evaluate the uncertainties induced by the incomplete knowledge of the EoS, a meta-modeling technique is used. It consists in generating a large set (100 millions) of models with fully independent model parameters using the strategy proposed in Refs. [15, 16]. The probability distribution of the parameters is evaluated in a Bayesian approach, by constraining energy and pressure in low density homogeneous matter from a many-body perturbation theory (MBPT) based on two and three-nucleon chiral EFT interactions at

N^3LO and generating band predictions in isospin-symmetric and neutron matter [17]. The priors are determined from nuclear phenomenology and a similar meta-modeling technique was already employed in Ref. [18].

The nuclear experimental and low density theoretical uncertainties can thus be translated into a confidence ellipse [19] for the crustal thickness and moment of inertia. This is shown by the "LD" correlation curve of Fig. 1 which anticipates our main result.

The predictions considering only the nuclear experimental constraints included as uncorrelated parameter set are labelled as "Prior" while the predictions from EoS models which further satisfy basic physical constraints at high density – see more details in the following – are labelled "HD". Fig. 1 shows that the "LD" prediction is considerably less dispersed than the "Prior" or "HD" ones. The 2σ surface of the complete (LD+HD) prediction including all constraints corresponds to a 84% confidence level [39], and the corresponding EoS is represented in the lower part of the Figure.

As discussed above, the crust properties require the knowledge of the crust-core transition density and pressure. They have been calculated by many authors using different versions of the density functional theory [11, 20]. Most calculations are based on the thermodynamical spinodal, while this method provides only a qualitative estimation of the crust-core transition [21–23]. Indeed, the transition occurs when the inhomogeneous phase becomes energetically favored over the homogeneous one [24], which is governed by the interplay between the surface tension and the Coulomb energy. As a matter of fact, none of these terms contribute to the thermodynamical spinodal. A better estimation is obtained from the so-called dynamical spinodal [25], which corresponds to the instability border with respect to finite size density fluctuations. Such calculations have however been performed for a small set of models [20–23].

Following Ref. [15], the generated meta-models are

	n_t (fm $^{-3}$)		P_t (MeV/fm 3)		$\rho_{c,1.4}$ ($\times 10^{14}$) (g/cm 3)		$R_{1.4}$ (km)		$l_{crust,1.4}$ (km)		$I_{crust,1.4}/I_{1.4}$ (%)	
	Average	σ	Average	σ	Average	σ	Average	σ	Average	σ	Average	σ
prior	0.089	0.037	0.310	0.340	6.661	1.102	12.77	0.61	1.13	0.29	3.40	3.34
HD	0.075	0.032	0.392	0.328	6.455	1.013	12.80	0.65	1.17	0.29	4.39	3.26
LD	0.074	0.011	0.364	0.122	7.820	1.075	11.94	0.42	0.95	0.11	3.54	1.33
LD+HD	0.077	0.010	0.389	0.111	6.756	0.606	12.47	0.25	1.03	0.10	4.50	1.25

TABLE I. Average value and standard deviation of the transition density n_t , transition pressure P_t , central mass density ρ_c , radius R , crust thickness l_{crust} , and crustal fraction of moment of inertia for a $1.4M_\odot$ neutron star for different filters. We impose $p = 3$.

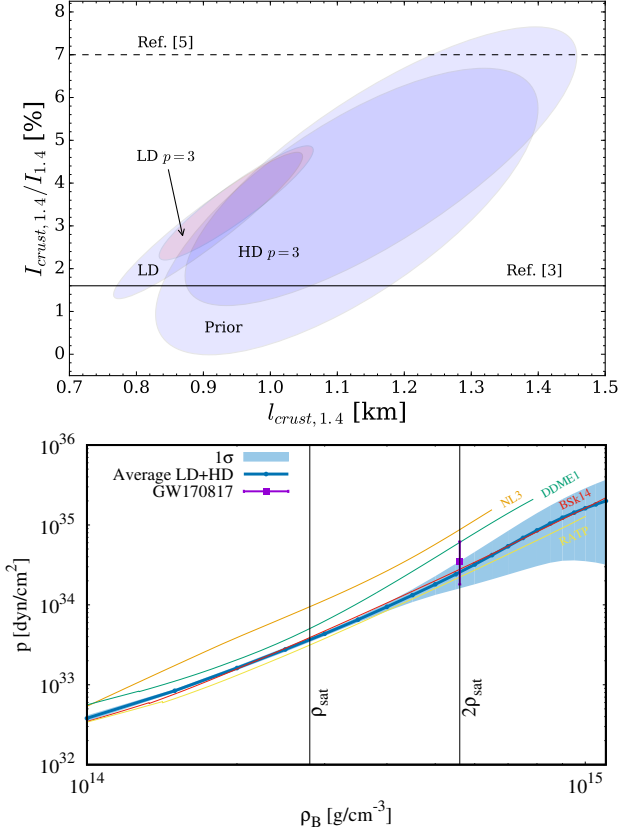


FIG. 1. (Color online) Top: 1σ confidence ellipse for the crust thickness l_{crust} and the fraction of crust moment of inertia I_{crust}/I for a $1.4M_\odot$ neutron star with different filters (see text). Minimal values needed to justify Vela glitches without [3] and with [5] entrainment are represented. Bottom: behavior of the equation of state retained by this study compared to some popular models. The recent constraint from GW170817 [10] is also given.

characterized by a set of empirical parameters $\{\vec{P}_\alpha\} = \{n_{sat}, K_{sat}, Q_{sat}, Z_{sat}, E_{sym}, L_{sym}, Q_{sym}, Z_{sym}, m^*, \Delta m^*, b\}$, corresponding to the successive density derivatives at saturation of the uniform matter binding energy in the isoscalar and isovector channels. They characterize the density dependence of the energy in symmetric matter, and of the symmetry energy. An expansion up to the fourth order is necessary and sufficient to guarantee an excellent reproduction of existing functionals up to $4n_{sat}$, where n_{sat} is the saturation density of nuclear matter [15]. Two additional parameters rule the density dependence of the effective mass m^* and the effective mass splitting Δm^* , and an extra b parameter enforces the correct behavior

at zero density. This last parameter measures the low density deviation from a Taylor expansion at saturation, and turns out to be completely uninfluential in this study (see Fig. 3 below).

In the neutron star crust, the meta-modeling is extended with a surface term, validated through comparisons with Thomas-Fermi calculations [26],

$$\sigma_s(x) = \sigma_0 \frac{2^{p+1} + b_s}{x^{-p} + b_s + (1-x)^{-p}}, \quad (1)$$

where x is the cluster proton fraction, see also Refs. [27, 28]. The crust composition is then variationally determined within the compressible liquid drop model (CLDM) approximation [13, 14, 24, 29].

The expression (1) for the surface tension requires three additional parameters. σ_0 and b_s are adjusted to reproduce experimental masses of spherical magic and semi-magic nuclei: $^{40,48}\text{Ca}$, $^{48,58}\text{Ni}$, ^{88}Sr , ^{90}Zr , $^{114,132}\text{Sn}$, and ^{208}Pb [40]. The isovector surface parameter p determines the behavior of the surface energy for extreme isospin values, and it cannot be determined from experiments. In the following, we consider two different choices: either a fixed value $p = 3$, as suggested in Ref. [27], or including p in the parameter set $\{\vec{P}_\alpha\}$.

For each set of uniform matter parameters $\{\vec{P}_\alpha\}$, our fit provides optimal values for σ_0 and b_s and the resulting χ^2 enters the Bayesian likelihood probability defined as,

$$p_{lik}(\{\vec{P}_\alpha\}) = \mathcal{N} e^{-\frac{1}{2}\chi^2(\{\vec{P}_\alpha\})} \prod_\alpha g(\{\vec{P}_\alpha\}), \quad (2)$$

where the functions g are flat priors corresponding to a fully uncorrelated parameter set, which range is taken from Ref. [16], and \mathcal{N} the normalization.

The posterior distribution is obtained by filtering the results of Eq. (2) imposing either physical constraints at high (supra-saturation) density (HD), or ab-initio EFT constraints at low (sub-saturation) density (LD), or both (LD+HD):

$$p_{post}(\{\vec{P}_\alpha\}) = p_{lik}(\{\vec{P}_\alpha\}) \delta(\mathcal{F}(\{\vec{P}_\alpha\}) - \mathcal{F}_0), \quad (3)$$

where \mathcal{F}_0 is the chosen filter. The HD filter corresponds to the set of constraints: (i) positive symmetry energy up to M_{max} , (ii) stability of the EoS, (iii) causality up to the maximum mass, (iv) compatibility with the maximum observed masses $M_{max} \gtrsim 2M_\odot$ [30, 31], see Ref. [16] for more details. The LD filter retains only the EoS passing through the uncertainty band of the MBPT calculations of symmetric and neutron matter by Drischler et al. [17]. Other calculations can be found

in Refs. [32–34], which provide comparable theoretical band predictions. The use of a symmetric matter constraint is however important for the determination of the crust thickness, because the transition is governed by isoscalar instabilities.

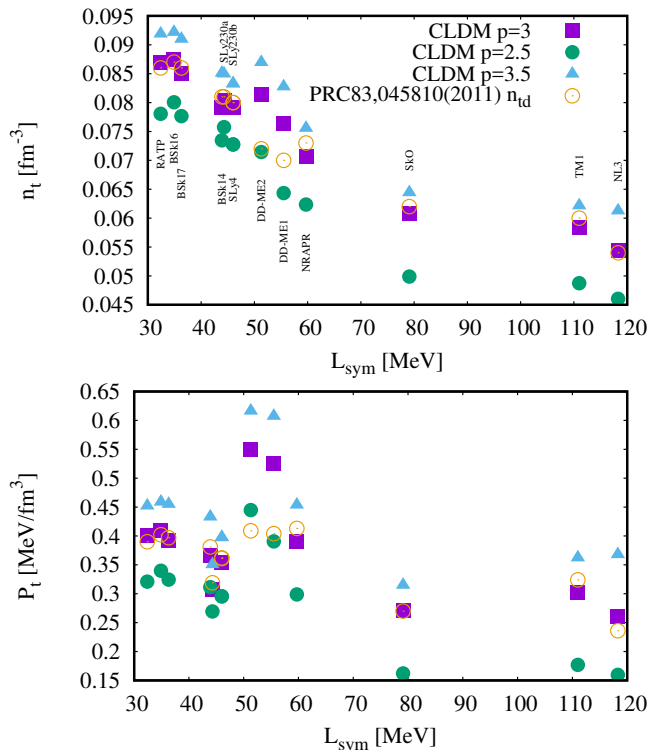


FIG. 2. (Color online) Transition density n_t (top) and transition pressure P_t (bottom) as a function of L_{sym} for several interactions. The empty dots (squares) are the transition points calculated in Ref. [20] using the dynamical spinodal. The filled circles, squares, and triangles corresponds respectively to our estimation of the transition points with $p = 2.5$, $p = 3$, and $p = 3.5$.

Note that the HD filter implicitly implies that first order phase transition does not occur in the star core up to $2M_{\odot}$, as the only hypothesis of the meta-modeling is the analyticity of the EoS [15]. Therefore, imposing the LD filter alone might also be physically acceptable, and we will consider the two filters separately in the following.

Table I gives the average values and the standard deviations, defined as

$$\langle X \rangle = \sum_{\{\vec{P}_{\alpha}\}} X(\{\vec{P}_{\alpha}\}) p(\{\vec{P}_{\alpha}\}), \quad (4)$$

for a set of observables X . Fixing $p = 3$, we consider different probability distributions: the uncorrelated prior distribution $p(\{\vec{P}_{\alpha}\}) = \prod_{\alpha} g(\vec{P}_{\alpha})$ (first line), or the posterior distribution Eq. (3) filtered according to the different constraints, $p(\{\vec{P}_{\alpha}\}) = p_{post}(\{\vec{P}_{\alpha}\})$, see rows 2 to 4. Knowing the transition point, a numerical solution of the TOV equation allows computing the star radius, the thickness of the crust, and the crustal moment of inertia [11, 35]. The first two moments of the distributions of these quantities are also reported in Table I

for a representative 1.4-solar mass neutron star. The results in Table I show that the high density constraints are essential to establish the average crustal properties, but the knowledge of the low density EoS is very constraining on the second moment of the distributions. Still, the transition pressure P_t and the fraction of crust moment of inertia have large uncertainties [36] of the order of 34% (resp. 37%) considering the LD probability, decreasing to about 28% (resp. 25%) if we additionally assume an analytical behavior of the EoS in the full density range covered by the observed neutron star (LD+HD, see last row in Table I).

The isovector surface parameter p plays an important role in the energetics of the inner crust [28], and may depart from its assumed value suggested in Ref. [27]. To determine a reasonable prior for p , we analyse its effect on the transition point. Fig. 2 displays the transition density and pressure obtained for a set of relativistic and non-relativistic functionals, in comparison with the dynamical spinodal calculation of Ref. [20]. We can see that values of the order $p \approx 3$ lead to a general good agreement with the instability analysis, and a variation ± 0.5 around $p = 3$ provides a good boundary for improved adjustment [41]. The impact of varying the isovector surface parameter $p = \{2.5, 3, 3.5\}$ is shown to be quite large in the 1σ confidence ellipse in Fig. 1.

Which empirical parameters contribute the most to the uncertainty in the observables shown in Fig. 1? To answer this question, the linear correlation coefficients $r_{XY} = \sigma_{XY}/(\sigma_X \sigma_Y)$ between I_{crust} and the empirical parameters $\{\vec{P}_{\alpha}\}$ are shown in Fig. 3. Very similar values for r_{XY} are found for the crustal thickness l_{crust} . We can see that isovector empirical parameters are far more influential than the isoscalar ones, as expected, E_{sym} , K_{sym} and Q_{sym} being the more influential parameters. The absence of correlation with the L_{sym} parameter deserves some comments. It is well known that the NS radius R is well correlated to L_{sym} [12, 35, 36]. The same is true for the core radius R_{core} , explaining why the correlations cancel in the crustal thickness $l_{crust} = R - R_{core}$ and consequently on $I_{crust,1.4}$. It then clearly appears that the higher order parameters beyond L_{sym} must be better constrained to improve the prediction of the crustal properties.

Fixing p tends to increase those correlations, as expected. However, if p is included in the parameter set, we can see that the uncertainty in the surface energy have an impact on the observables shown in Fig. 3 comparable to the one of the empirical parameters, see LD row. This is a new feature which has not been reported by previous analyses.

Fig. 3 also shows the correlation coefficients between observables. Large correlations are observed for the transition density and pressure, as expected from previous studies, e.g. Ref. [11], and the correlation between $l_{crust,1.4}$ and $I_{crust,1.4}$ is also found to be very large, see Fig. 1.

Finally, we show in Fig. 4 the full impact of our present knowledge on the relation between the glitch amplitude and the neutron star mass and radius. One- σ confidence ellipses for three different pulsars estimated from the observed glitch amplitude from Ref. [38] are given in the upper part of the fig-

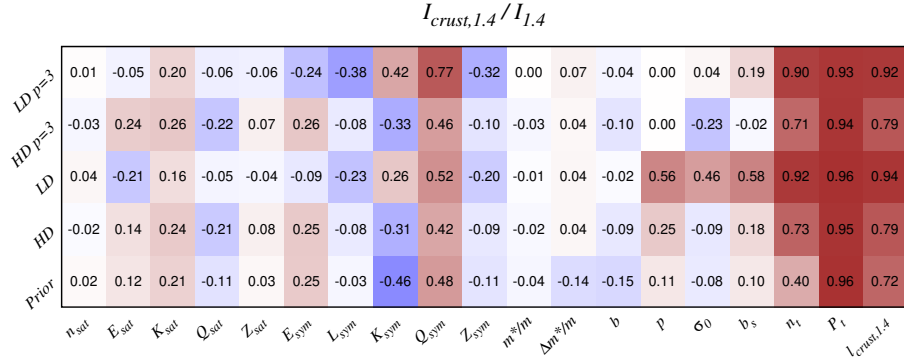


FIG. 3. (Color online) Correlation between the fraction of crust moment of inertia I_{crust}/I for a $1.4M_{\odot}$ neutron star and several parameters for different filters. The red (blue) color scale gives the intensity of the positive (negative) correlation, and the correlation coefficient is explicitly given for each parameter.

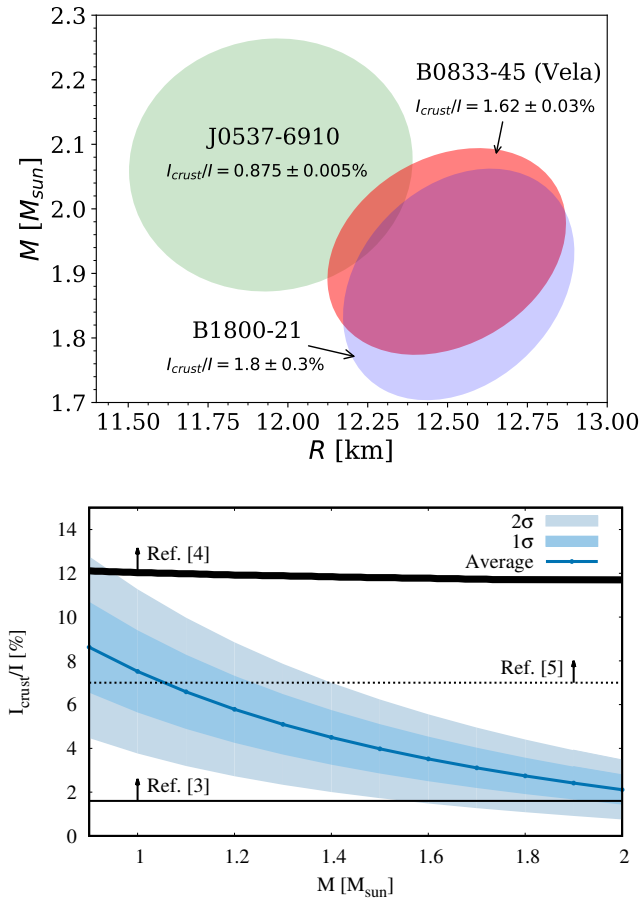


FIG. 4. (Color online) Top: 1σ confidence ellipse with the LD+HD $p = 3$ filter for the mass and radius of different pulsars estimated from the observed glitch amplitude from Ref. [38], without crustal entrainment. Bottom: average fraction of crust moment of inertia I_{crust}/I as a function of the mass. The 1σ and 2σ confidence regions are represented, as well as the minimum values needed to justify Vela glitches, with [4, 5] and without [3] crustal entrainment.

ure. Note that an innovative method was proposed to determine the mass and radius using observations of the maximum observed glitches [37]. It would be interesting to compare this approach with ours. The lower part gives a complete study of

the effect of entrainment in the case of Vela: the average value of the fraction of crust moment of inertia I_{crust}/I is shown, as well as the boundaries of the 1σ and 2σ probabilities. The different black lines represent the values proposed with [4, 5] and without [3] entrainment effect on the crust moment of inertia to explain Vela glitches. From Fig. 4 we can conclude that the value determined for the maximal entrainment effect is incompatible with the present nuclear physics knowledge.

In conclusion, considering the experimental and EFT theoretical predictions at low density, the uncertainty on the crust thickness (relative moment of inertia) is of the order of 9% (25%), for $M = 1.4M_{\odot}$. These uncertainties originate from the dispersion in the predictions of the crust-core transition point, which in turn depends on the high order isovector empirical parameters K_{sym} and Q_{sym} , as well as on the isovector surface energy parameter p . Higher precision in the experimental determination of K_{sym} and Q_{sym} , in the low density EFT theoretical predictions, and in the microscopic modeling of the surface energy at extreme isospin ratios are needed to reduce the uncertainties of crustal observables.

This work was partially supported by the IN2P3 Master Project MAC, "NewCompStar" COST Action MP1304, PHAROS COST Action MP16214.

-
- [1] C.M.Espinoza, A.G. Lyne, B.W. Stappers, M. Kramer, MNRAS 414, 1679 (2011).
 - [2] B. Haskell and A. Melatos, Int. J. Mod. Phys. D 24, 1530008 (2015).
 - [3] B. Link, R. I. Epstein, and J. M. Lattimer, Phys. Rev. Lett. 83, 3362 (1999).
 - [4] T. Delsate, N. Chamel, N. Gurlebeck, A. F. Fantina, J. M. Pearson, and C. Ducoin, Phys. Rev. D 94, 023008 (2016).
 - [5] N. Andersson, K. Glampedakis, W. C. G. Ho, and C. M. Espinoza, Phys. Rev. Lett. 109, 241103 (2012).
 - [6] N. Martin and M. Urban, Phys. Rev. C 94, 065801 (2016).
 - [7] G. Watanabe and C. J. Pethick, Phys. Rev. Lett. 119, 062701 (2017).
 - [8] D. Page and S. Reddy, Phys. Rev. Lett. 111, 241102 (2013).
 - [9] W. G. Newton, J. Hooker, M. Gearheart, K. Murphy, D-H Wen,

- F. J. Fattoyev, and B-A Li, *Eur. Phys. Journ. A* 50 (2014) 41.
- [10] B.P.Abbot et al., *Phys. Rev. Lett.* 121 (2018) 161101.
- [11] J. Piekarewicz, F. J. Fattoyev, and C. J. Horowitz, *Phys. Rev. C.* 90, 015803 (2014).
- [12] M. Fortin, C. Providência, Ad. R. Raduta, F. Gulminelli, J. L. Zdunik, P. Haensel, and M. Bejger, *Phys. Rev. C* 94, 035804 (2016).
- [13] B.K. Sharma, M. Centelles, X. Vias, M. Baldo and G.F. Burgio (2015) *Astron. Astrophys.* 584, A103.
- [14] H. Shen, H. Toki, K. Oyamatsu and K. Sumiyoshi (1998) *Nucl. Phys.* A637 435.
- [15] J. Margueron, R. Hoffmann Casali, and F. Gulminelli, *Phys. Rev. C* 97, 025805 (2018).
- [16] J. Margueron, R. Hoffmann Casali, and F. Gulminelli, *Phys. Rev. C* 97, 025806 (2018).
- [17] C. Drischler, K. Hebeler, and A. Schwenk, *Phys. Rev. C* 93, 054314 (2016).
- [18] A. W. Steiner, J. M. Lattimer, and E. F. Brown, *Astrophys. J. Lett.* 765, 5 (2013).
- [19] M.Friendly, G.Monette and J.Fox, *Statistical Science* vol.28, No.1, 1 (2013).
- [20] For a compilation of different relativistic and non-relativistic approaches, see C. Ducoin, J. Margueron, C. Providencia, and I. Vidana, *Phys. Rev. C* 83, 045810 (2011).
- [21] H.Pais, A.Sulaksono, B.K.Agrawal, C.Providencia, *PRC*93(2016)045802
- [22] C. Ducoin, P. Chomaz, and F. Gulminelli, *Nucl. Phys. A* 789, 403 (2007).
- [23] J. Xu, L.-W. Chen, B.-A. Li, and H.-R. Ma, *Astrophys. J.* 697, 1549 (2009).
- [24] G. A. Baym, H.A. Bethe and C. J. Pethick, *Nucl. Phys. A* 15 (1971) 225.
- [25] C.J.Pethick, D.G.Ravenhall, C.P.Lorentz, *Nucl. Phys. A*584 (1995) 675.
- [26] D.G. Ravenhall, C.J. Pethick, and J.M. Lattimer, *Nucl. Phys. A* 407, 571 (1983).
- [27] C.P. Lorenz, D.G. Ravenhall, and C.J. Pethick, *Phys. Rev. Lett.* 70 (1993) 379
- [28] W.G.Newton, M.Gearheart and B-A Li *The Astrophysical Journal Supplement Series* 204(1), DOI: 10.1088/0067-0049/204/1/9, (2013).
- [29] F. Douchin, and P. Haensel, *A&A*, 380 (2001) 151
- [30] J. Antoniadis, P. Freire, N. Wex, et al., *Science* 340, 1233232 (2013).
- [31] Z. Arzoumanian, A. Brazier, S. Burke-Spolaor et al., *Astro. J. Suppl. Series* 235, 37 (2018).
- [32] I. Tews, S. Gandolfi, A. Gezerlis, A. Schwenk, *Phys. Rev. C* 93, 024305 (2016).
- [33] J.W. Holt, N. Kaiser, T.R. Whitehead, *Phys. Rev. C* 97, 054325 (2018).
- [34] I. Tews, J. Calson, S. Gandolfi, S. Reddy, *The Astro. J.* 860, 149 (2018).
- [35] J.M. Lattimer, M. Prakash, *Phys. Rep.* 333 (2000) 121.
- [36] A. W. Steiner, S. Gandolfi, F. J. Fattoyev, and W. G. Newton, *Phys. Rev. C* 91 (2015) 015804.
- [37] P.M. Pizzochero, M. Antonelli, B. Haskell, and S. Seveso, *Nature Astronomy* 1, 0134 (2017).
- [38] W.C.G.Ho, C.M.Espinoza, D.Antonopoulou, N.Andersson, *Sci. Adv.*1 (2015) e1500578.
- [39] This value deviates from the standard 90% because of non-gaussianity of the probability distribution.
- [40] Enlarging the set of mass data does not modify the results.
- [41] In the case of the SLy4 functional, the value $p = 2.61$ is needed to reproduce the unified EoS approach by Douchin and Haensel [29].